NASA TECHNICAL MEMORANDUM

NASA TM X-2726

NASA TM X-2726

CASE FILE COPY

MEASUREMENT OF GASEOUS EMISSIONS FROM AN AFTERBURNING TURBOJET ENGINE AT SIMULATED ALTITUDE CONDITIONS

by Larry A. Diehl

Lewis Research Center

Cleveland, Ohio 44135

NATIONAL AERONAUTICS AND SPACE ADMINISTRATION • WASHINGTON, D. C. • MARCH 1973

1. Report No.	2. Government Accession No.	3. Recipient's Catalog No.
NASA TM X-2726		

4. Title and Subtitle	5. Report Date
MEASUREMENT OF GASEOUS EMISSIONS FROM AN AFTERBURNING TURBOJET ENGINE AT SIMULATED ALTITUDE CONDITIONS	March 1973
	6. Performing Organization Code
7. Author(s)	8. Performing Organization Report No.
Larry A. Diehl	E-7238
	10. Work Unit No.
9. Performing Organization Name and Address	501-24
Lewis Research Center National Aeronautics and Space Administration Cleveland, Ohio 44135	11. Contract or Grant No.
	13. Type of Report and Period Covered
12. Sponsoring Agency Name and Address	Technical Memorandum
National Aeronautics and Space Administration Washington, D.C. 20546	14. Sponsoring Agency Code

15. Supplementary Notes

16. Abstract

Gaseous emissions from a J85-GE-13 turbojet engine were measured over a range of fuel-air ratios from idle to full afterburning and simulated altitudes from near sea-level to 12 800 meters (42 000 ft). Without afterburning, carbon monoxide and unburned hydrocarbon emissions were highest at idle and lowest at takeoff; oxides of nitrogen exhibited the reverse trend. With afterburning, carbon monoxide and unburned hydrocarbon emissions were greater than for military power. Carbon monoxide emissions were altitude dependent. Oxides of nitrogen emissions were less at minimum afterburning than at military power. For power levels above minimum afterburning, the oxides of nitrogen emissions were both power level and altitude dependent.

17. Key Words (Suggested by Author(s))	18. Distribution Statement
Air pollution; Afterburning; Combustion; Combustion products; Exhaust gases; Exhaust products; Fuel combustion; Jet engines; Gas turbine engines; Thrust augmentation	Unclassified - unlimited

19. Security Classif. (of this report)	20. Security Classif. (of this page)	21. No. of Pages	22. Price*
Unclassified	Unclassified	19	$3.00

* For sale by the National Technical Information Service, Springfield, Virginia 22151

MEASUREMENT OF GASEOUS EMISSIONS FROM AN AFTERBURNING TURBOJET ENGINE AT SIMULATED ALTITUDE CONDITIONS

by Larry A. Diehl

Lewis Research Center

SUMMARY

Gaseous emissions from a J85-GE-13 turbojet engine were measured over a range of fuel-air ratios from idle to full afterburning and simulated altitudes from near sea-level to 12 800 meters (42 000 ft). Gas samples were collected at the afterburner exit and were analyzed for carbon monoxide, unburned hydrocarbons, oxides of nitrogen, and carbon dioxide.

Without afterburning, carbon monoxide and unburned hydrocarbon emissions were highest at idle and lowest at takeoff; oxides of nitrogen exhibited the reverse trend. At military throttle setting, increasing altitude results in increasing CO emissions.

With afterburning, carbon monoxide and unburned hydrocarbon emissions were greater than for military power. As augmentation was increased to maximum afterburning, carbon monoxide emissions rose while unburned hydrocarbons decreased. An altitude dependence on carbon monoxide production was observed. Oxides of nitrogen emissions were less at minimum afterburning than at military power. For power levels above minimum afterburning, the oxides of nitrogen emissions tended to increase with power level and decrease with altitude.

INTRODUCTION

The purpose of this report is to document the gaseous emissions from an afterburning turbojet engine at various simulated altitudes. Particular emphasis was placed on measurement of the oxides of nitrogen.

Stimulated by the enactment of the Clean Air Act, a good deal of information has been gathered concerning the current emission levels of aircraft turbine engines. A large compilation of data may be found in reference 1. The bulk of the data obtained to date has been taken at ground level, static engine conditions. The primary purpose of

these data is to assess the environmental impact of pollutant emissions in the vicinity of the airport.

A limited amount of data is available concerning the effect of afterburning on engine emissions (refs. 2 to 5). Concern about the environmental effect of the supersonic transport has generated a need for emission data for afterburning engines at altitude conditions. The effect of altitude was studied in references 2 and 3.

Experimental results from a previous study at the Lewis Research Center (ref. 2) indicated that the level of oxides of nitrogen emitted from an afterburning engine is determined by the primary combustor. This result was later substantiated by data gathered at the Naval Air Propulsion Test Center (ref. 3). The present study examines the gaseous emissions from a different turbojet engine, with emphasis on the oxides of nitrogen emissions.

Measurements of engine exhaust emissions were made on a J85-GE-13 turbojet engine with afterburner tested in an altitude test cell. The test conditions included both afterburning and nonafterburning power levels at simulated altitudes to 12 800 meters (42 000 ft). All tests were conducted using ASTM A-1 fuel. Samples were continuously analyzed for oxides of nitrogen, unburned hydrocarbons, carbon monoxide, and carbon dioxide.

APPARATUS

Engine

The J85-GE-13, shown in figure 1, is an afterburning turbojet engine consisting of an eight-stage, axial-flow compressor directly coupled to a two-stage turbine, an annular combustor, an afterburner, and a variable-area primary exhaust nozzle. The engine has a rated sea-level static thrust of 12 100 newtons (2720 lb) at military power and 18 150 newtons (4080 lb) at maximum afterburning. The compressor has an overall total pressure ratio of 6.9 and a rated airflow of 20 kilograms per second (44 lb/sec) at a rated rotor speed of 16 500 rpm.

The afterburner consists of a diffuser, a single V-gutter combination flameholder and pilot burner, and an afterburner and pilot burner fuel-injection system. There are 16 afterburner and 4 pilot burner fuel spray bars. The variable-area primary nozzle consists of 12 overlapping leaves and seals actuated in unison by three hydraulic actuators.

The integrated fuel system consists of a main and an afterburner fuel control and is operated by a single power lever. The main fuel control operates as a function of compressor inlet temperature, compressor discharge static pressure, engine rotor speed, and the power lever angle. The afterburner fuel control operates as a function of com-

pressor discharge static pressure and the power lever angle. Exhaust nozzle area is a function of power lever angle and a predetermined limit for turbine discharge temperature. A detailed description of the engine components may be found in reference 6.

Facility

The engine was installed in the Propulsion Systems Laboratory Altitude Chamber at Lewis. This facility is capable of simulating altitudes from sea level to 24 000 meters (80 000 ft) at airflow rates of 220 and 23 kilograms per second (480 and 50 lb/sec), respectively. Air handling equipment is available to supply sufficient flow rates at pressures and temperatures necessary to simulate the Mach number range from static to 1.5 at sea level. The thrust stand was not used for these tests, and no measurement of efficiency was made.

The engine was instrumented to record and monitor the engine operating parameters. The measurements were recorded on the Lewis central automatic digital data encoder (CADDE). The types and location of instrumentation are discussed in reference 7.

Gas Sample Probes

Two fixed position, water cooled, stainless-steel gas sample probes were used. The first probe, shown in figure 2, was sized to sample a flow area equal to the nozzle area at maximum afterburning. The second probe was sized to correspond to the nozzle area at military throttle setting. Ten sampling points, corresponding to centers of equal area, were common manifolded within the probe. By interchanging probes, and operating over a range of engine conditions, it was hoped that some information could be gained regarding the importance of correctly sized probes on sample accuracy. The probe was located about 15 centimeters (6 in.) downstream of the nozzle.

Gas Sample System

Approximately 9 meters (30 ft) of 0.95 centimeter (3/8-in.) stainless-steel line was used to transport the sample to the analytical instruments. In order to prevent condensation of water and to minimize adsorption-desorption effects of hydrocarbon compounds, the line was heated with steam at 428 K (310° F). For the majority of test conditions a heated metal bellows pump was required to supply sufficient pressures,

69 kN/m^2 (10 psig), to operate the analytical instruments. At the higher simulated altitude conditions the pump capacity was sufficient to provide a line residence time of about 5 seconds, while at lower simulated altitudes the line residence time was about 1 second.

The exhaust gas analysis system (fig. 3) is a packaged unit consisting of four commercially available instruments along with associated peripheral equipment necessary for sample conditioning and instrument calibration. In addition to visual readout, electrical inputs are provided to the IBM 360 computer for on-line analysis and evaluation of the data.

The hydrocarbon content of the exhaust gas is determined by a Beckman Instruments Model 402 Hydrocarbon Analyzer. This instrument is of the flame ionization detector type.

The concentration of the oxides of nitrogen is determined by a Thermo Electron Corporation Model 10A Chemiluminescent Analyzer. The instrument includes a thermal convertor to reduce NO_2 to NO and was operated at 973 K (1290^o F).

Both carbon monoxide and carbon dioxide analyzers are of the nondispersive infrared (NDIR) type (Beckman Instruments Model 315B). The CO analyzer has four ranges: 0 to 100 ppm, 0 to 1000 ppm, 0 to 1 percent, and 0 to 10 percent. This range of sensitivity is accomplished by using stacked cells of 0.64- and 33-centimeter (0.25- and 13.5-in.) length. The CO_2 analyzer has two ranges, 0 to 5 percent and 0 to 15 percent, with a sample cell length of 0.32 centimeter (0.125 in.).

ANALYTICAL PROCEDURE

All analyzers were checked for zero and span prior to the test. Since the analyzer console requires only a few seconds for each instrument to switch from calibration to sample modes, it was possible to perform frequent checks to insure the calibration accuracy without disrupting testing.

Where appropriate, the measured quantities were corrected for water vapor removed. The correction includes both inlet air humidity and water vapor from combustion. The equations used are given in reference 8.

The emission levels of all the constituents were converted to an emission index (EI) parameter. The EI may be computed from the measured quantities as proposed in reference 8, or an alternate procedure is to use the metered fuel-air ratio, when this is accurately known. Using the latter scheme the EI for any constituent X is given by

$$EI_X = \frac{M_X}{M_A} \frac{1+f}{f} [X] \times 10^{-3}$$

where

EI_X emission index in grams of X/kg of fuel burned

M_X molecular weight of X

M_e average molecular weight of exhaust gas

f metered fuel-air ratio

[X] measured concentration of X, ppm

Both procedures yield identical results when the sample validity is good.

TEST CONDITIONS

The engine test conditions are presented in table I. Facility limitations prohibit the operation of the engine with the altitude chamber at atmospheric pressure, thus true "sea level" readings were not obtained. With the exception of engine idle, the lowest simulated altitude was approximately 1830 meters (6000 ft). At each of the pressure simulated altitude conditions, the engine was operated at military, minimum afterburning, intermediate afterburning, and maximum afterburning throttle settings.

The two different sampling probes were used in the following manner: The raked sized for military throttle setting was used at military, minimum afterburning, intermediate afterburning, and three low-power throttle settings. The rake sized for maximum afterburning was used at intermediate afterburning, maximum afterburning, and two low-power throttle settings.

RESULTS AND DISCUSSION

The emission data obtained during the test program are presented in table II. Values of emission index (EI) were computed from the total fuel flow (engine plus afterburner) and the metered air flow.

Carbon Monoxide Emissions

The values of carbon monoxide emission index are shown in figure 4 as a function of the total engine fuel-air ratio. As the engine throttle is advanced from idle to military, the carbon monoxide EI decreases markedly. Both size probes were used at low power settings (idle, 30 percent) since these settings can be closely duplicated after changing

probes. The measured CO emissions were nearly identical. This result is significant because analysis of the data of reference 1 indicated that the potential for sampling errors at idle power was considerable.

At military throttle, a four-to-one increase in the CO emission is observed as the altitude is increased. Due to the limited amount of data, it is difficult to accurately draw curves showing the altitude dependence of carbon monoxide EI with afterburner operation. However, even if the location of the curves is not well resolved, the trend with altitude is unmistakable. Increasing altitude results in increasing afterburner CO emission. An altitude dependence cannot be inferred from the data of reference 3.

It is difficult to determine if any differences in sampling exist between the two probes at intermediate afterburning. Since the fuel-air ratio at this condition was not exactly duplicated when the probes were interchanged, the slight reduction in CO may be due either to sampling, or to the change in engine operating conditions. Some differences were noted when the sample rake was moved downstream. A significant reduction in CO with axial probe placement occurred at the 1830-meter (6000-ft) altitude.

The measured CO values comprise an expected upper limit. Particularly for the afterburning cases, the exhaust plume is of high enough temperature that continuing oxidation may occur downstream of the sample probe.

Unburned Hydrocarbon Emissions

The flame ionization detector used to measure unburned hydrocarbons is calibrated to count carbon atoms, and the results are expressed as parts per million carbon (ppm C). In order to calculate a value for the emission index it is necessary to make some assumption as to the structure of the unburned hydrocarbon molecule. The assumed form was CH_2.

The unburned hydrocarbon data are presented in figure 5. Hydrocarbons decrease rapidly as the throttle is advanced from idle to military. The variation in emission level at military throttle is due to data scatter involved in making measurements at the 5 ppm level. No altitude dependence on hydrocarbons was discernible. The general trend and emission level of the afterburner data is in agreement with the data of references 2 and 3. The hydrocarbon levels decreased when the probe was moved downstream.

Oxides of Nitrogen Emissions

The values of the oxides of nitrogen emission index are presented in figure 6. The nonafterburning No_x emissions exhibit an interesting trend in that the maximum value

occurs at an intermediate power setting. This phenomena will be discussed later in the report. In agreement with previous afterburning engine studies (refs. 2 and 3), the maximum overall NO_x emission index level is determined by the primary combustor. At military and afterburning throttle settings operation at increased altitude results in decreased NO_x emissions. Note that moving the probe downstream resulted in an increase in the measured emission values.

Additional information concerning the effect of the afterburner can be obtained by examining the data expressed in ppm. Figure 7 shows that the general trend with fuel-air ratio is to increase the volumetric concentration. However, a very important exception occurs at the onset of afterburning where the NO_x level is actually lower than at military power.

Reduction of NO_x by CO is not a viable explanation since, if this were occurring, the largest decrease in NO_x would be expected at the highest afterburner fuel-air ratios where CO levels are greatest (fig. 4). This is in conflict with the observed NO_x trends. Furthermore, reduction of the NO_x by CO does not appear kinetically possible as a gas phase reaction. It is possible that the NO_x may combine with the unburned hydrocarbons which exist in large amounts at this condition (fig. 5).

The effect of alititude and the effect of axial probe location are the same as shown on the previous figure. In addition, it appears that differences between the two sample probes are minor since agreement is good both at idle and intermediate afterburning.

Figure 8 shows the nitrogen dioxide concentration as a function of total fuel-air ratio. For nonafterburning operation, the NO_2 concentration is maximum at an intermediate power setting. This is similar to the behavior of the Spey engine data reported in reference 9. With afterburning it is difficult to determine a consistent trend with altitude due to data scatter.

It is felt that the line residence time of a few seconds is too short for the oxidation of NO to NO_2 to be of any consequence. Therefore, the decrease in NO_x from military to minimum afterburning shown in figures 6 and 7 must be due to a decrease in the nitric oxide concentration since the NO_2 concentration increases (fig. 8).

Figure 9 shows the nitrogen dioxide fraction of the total oxides of nitrogen. At idle, the oxides of nitrogen consist entirely of NO_2. As the throttle is increased to military power setting, the NO_2 fraction drops to the 20 to 30 percent level. This trend is in good agreement with the data presented in reference 9 for several commercial aviation jet engines. With the onset of afterburning, the NO_2 fraction is increased. Some altitude dependence is again observed while afterburning. With increasing altitude the fraction of NO_2 is increased. The slight axial displacement of the probe results in a reduced fraction of NO_2.

SAMPLE VALIDITY

The measured values of CO, CO_2, and unburned hydrocarbon were used to compute an emission based fuel-air ratio, and this value was compared with the metered fuel-air ratio. The emission based fuel-air ratio is computed by the method suggested in reference 8. Results of this computation are shown in figure 10. With the exception of three points, the data group within ±10 percent. The three points in question were not discarded because the observed discrepancy is believed due to errors in fuel flow measurement.

The general problem of sample validity is still not completely resolved. Even though the carbon balance shows good sample validity, afterburner combusion efficiency inferred from the gas sample appears to be somewhat high. Nonafterburning efficiencies calculated in this manner appear correct.

SUMMARY OF RESULTS

Gaseous emissions from a J85-GE-13 turbojet engine were measured over a range of fuel-air ratios from idle to full afterburning and simulated altitudes from near sea level to 12 800 meters (42 000 ft). Engine inlet temperature was constant at 294 K (530° R).

Pollutant emissions obtained for carbon monoxide, unburned hydrocarbons, and oxides of nitrogen gave the following results:

1. Without afterburning, carbon monoxide emissions were highest at idle and decreased to their minimum level at military throttle. With afterburning, CO emissions were increased, and at maximum afterburning the levels exceeded those obtained at idle. Carbon monoxide emissions are altitude dependent with increasing altitude causing increased emissions.

2. For nonafterburning modes unburned hydrocarbon emissions are highest at idle and lowest at military throttle. In the afterburning modes, emission levels are highest at minimum afterburning and decrease to maximum afterburning. There appears to be little effect of altitude.

3. Without afterburning, the minimum emission level of oxides of nitrogen occured at idle, while the maximum value occured at an intermediate power setting. For all afterburning power levels, NO_x emission index levels were less than those produced by the primary combustor alone. At minimum afterburner the volumetric concentration of NO_x was less than at military power indicating that, by some mechanism, the NO_x was decreased. While a complete explanation is not available for this occurrence, the greatest decrease takes place when the unburned hydrocarbons are maximum. Emission

levels are lowest at minimum afterburning and increase to maximum afterburning. However, this effect is offset by the effect of altitude which tends to decrease the concentration of oxides of nitrogen as altitude is increased. At idle the NO_x consists entirely of NO_2, while at military throttle the NO_x consists of about 25 percent NO_2. With the onset of afterburning the fraction of NO_x as NO_2 is about 70 percent and tends to decrease with increasing afterburner fuel-air ratio. At a given fuel-air ratio the NO_2/NO fraction is highest at the highest altitude and decreases as altitude decreases.

Lewis Research Center
National Aeronautics and Space Administration,
Cleveland, Ohio, November 28, 1972,
501-24.

REFERENCES

1. Bogden, Leonard; and McAdams, H. T.: Analysis of Aircraft Exhaust Emission Measurements. Rep. NA-5007-K-1, Cornell Aeronautical Lab., Inc., Oct. 1971.

2. Diehl, Larry A.: Preliminary Investigation of Gaseous Emissions from Jet Engine Afterburners. NASA TM X-2323, 1971.

3. Palcza, J. Lawrence: Study of Altitude and Mach Number Effects on Exhaust Gas Emissions of an Afterburning Turbofan Engine. Rep. FAA-RD-72-31, AD-741249, 1971.

4. Crawford, L. W.; Mason, A. A.; and Lents, J. M.: Pollutant Production in a Simulated Turbojet Afterburner. Part I: Experimental and Theoretical Study. Tennessee Univ. (AFAPL-TR-71-66, P. I, AD-739176) Feb. 1972.

5. Lazalier, G. R.; and Gearhart, J. W.: Measurement of Pollutant Emissions from an Afterburning Turbojet Engine at Ground Level II. Gaseous Emissions. Rep. AEDC-TR-72-70, ARD, Inc., Aug. 1972.

6. Anon.: Installation Manual - J85-GE-13. Rep. SEI-195, General Electric Co., Aug. 1964.

7. Antl, Robert J.; and Burley, Richard R.: Steady-State Airflow and Afterburning Performance Characteristics of Four J85-GE-13 Turbojet Engines. NASA TM X-1742, 1970.

8. Anon.: Procedure for the Continuous Sampling and Measurement of Gaseous Emissions from Aircraft Turbine Engines. ARP-1256, SAE, Oct. 1971.

9. Cox, F. W.; Penn, F. W.; and Chase, J. O.: A Field Survey of Emissions from Aircraft Turbine Engines. Rep. BM-RI-7634, U.S. Bureau of Mines, 1972.

TABLE I. - ENGINE TEST CONDITIONS

[Engine inlet temperature, 294 K (70° F).]

Test condition	Engine inlet total pressure		Altitude chamber static pressure		Simulated altitude	
	kN/m^2	psia	kN/m^2	psia	m	ft
Idle	102.1	14.8	91.0	13.2	-----	-----
30 Percent power	104.2	15.1	79.3	11.5	1 980	6 500
85 Percent power	104.2	15.1	79.3	11.5	1 980	6 500
Altitude	104.2	15.1	82.1	11.9	1 830	6 000
Altitude	85.5	12.4	54.5	7.9	4 880	16 000
Altitude	56.6	8.2	36.6	5.3	7 620	25 000
Altitude	25.5	3.7	16.6	2.4	12 800	42 000

TABLE II. - MEASURED GASEOUS EMISSIONS FOR J85-GE-13 ENGINE

All emission corrected for H_2O removed.

Test condition	Altitude, m	Airflow, kg/sec	Total fuel-air ratio	NO_x			CO		HC		Sample rake used
				NO ppm	NO_x ppm	g/kg fuel	ppm	g/kg fuel	ppm C	g/kg fuel	
Idle	-----	7.8	0.0062	0	9	2.3	1 203	188.4	643	50.4	Maximum
Idle	-----	8.3	.0064	0	10	2.49	1 157	175.6	702	53.3	Military
30 Percent power	1 980	16.9	.0077	2.5	18	3.76	373	47.1	74	4.7	Military
30 Percent power	1 980	16.6	.0071	5	19	4.32	369	50.5	64	4.4	Maximum
85 Percent power	1 980	21.4	.0143	37	58	6.52	243	16.6	10	.34	Military
Military	1 830	21.7	.0178	39	52	4.74	290	16.0	4	.10	
Military	4 880	18.1	.0178	40	53	4.82	340	18.8	2	.04	
Military	7 620	11.7	.0179	36	48	4.34	521	28.6	2	.05	
Military	12 800	4.8	.0168	25	36	3.50	1 065	62.2	6	.17	
Minimum A/B	1 830	21.4	.0342	17	44	2.12	1 509	44.0	5250	76.7	
Minimum A/B	4 880	18.0	.0266	11	28	1.71	1 963	73.1	2288	42.6	
Minimum A/B	7 620	11.7	.0238	8	32	2.15	1 732	71.9	1488	30.9	
Minimum A/B	12 800	4.9	.0295	6	32	1.79	2 418	81.4	1368	23.0	
Intermediate A/B	1 830	21.6	.0388	18	62	2.65	1 901	49.1	621	8.0	
Intermediate A/B	1 830	21.4	.0463	45	73	2.61	1 838	40.1	113	1.2	Maximum
Intermediate A/B	1 830	21.4	.0455	63	92	3.34	1 276	28.3	35	.38	Maximum[a]
Intermediate A/B	4 880	17.2	.0423	23	60	2.36	2 184	51.9	260	3.09	Maximum
Intermediate A/B	4 880	18.0	.0381	17	58	2.51	2 465	64.8	998	13.1	Military
Intermediate A/B	7 620	11.9	.0375	9	46	2.02	3 292	87.9	1628	21.8	Military
Intermediate A/B	7 620	11.2	.0448	11	50	1.83	3 455	77.8	459	5.17	Maximum
Intermediate A/B	12 800	4.7	.0436	5	29	1.12	6 729	155.6	1265	14.6	Maximum
Intermediate A/B	12 800	4.9	.0387	5	30	1.26	4 562	118.1	2917	37.8	Military
Maximum A/B	1 830	21.2	.0683	87	104	2.58	13 690	206.6	11	.08	Maximum
Maximum A/B	1 830	21.0	.0560	70	112	3.35	7 386	134.4	67	.61	Maximum
Maximum A/B	1 830	21.1	.0544	87	116	3.58	4 038	75.5	7	.07	Maximum[a]
Maximum A/B	4 880	17.5	.0579	68	98	2.84	14 463	225.0	28	.25	Maximum
Maximum A/B	4 880	17.8	.0574	90	116	3.39	16 775	298.2	9	.08	Maximum[a]
Maximum A/B	7 620	11.3	.0604	43	78	2.17	27 953	473.5	69	.59	Maximum
Maximum A/B	12 800	4.7	.0654	10	40	1.04	47 008	738.9	1732	13.6	Maximum
Maximum A/B	12 800	4.8	.0661	40	65	1.66	45 899	714.4	125	.98	Maximum[a]

[a]Maximum rake moved 0.3 m (1 ft) back.

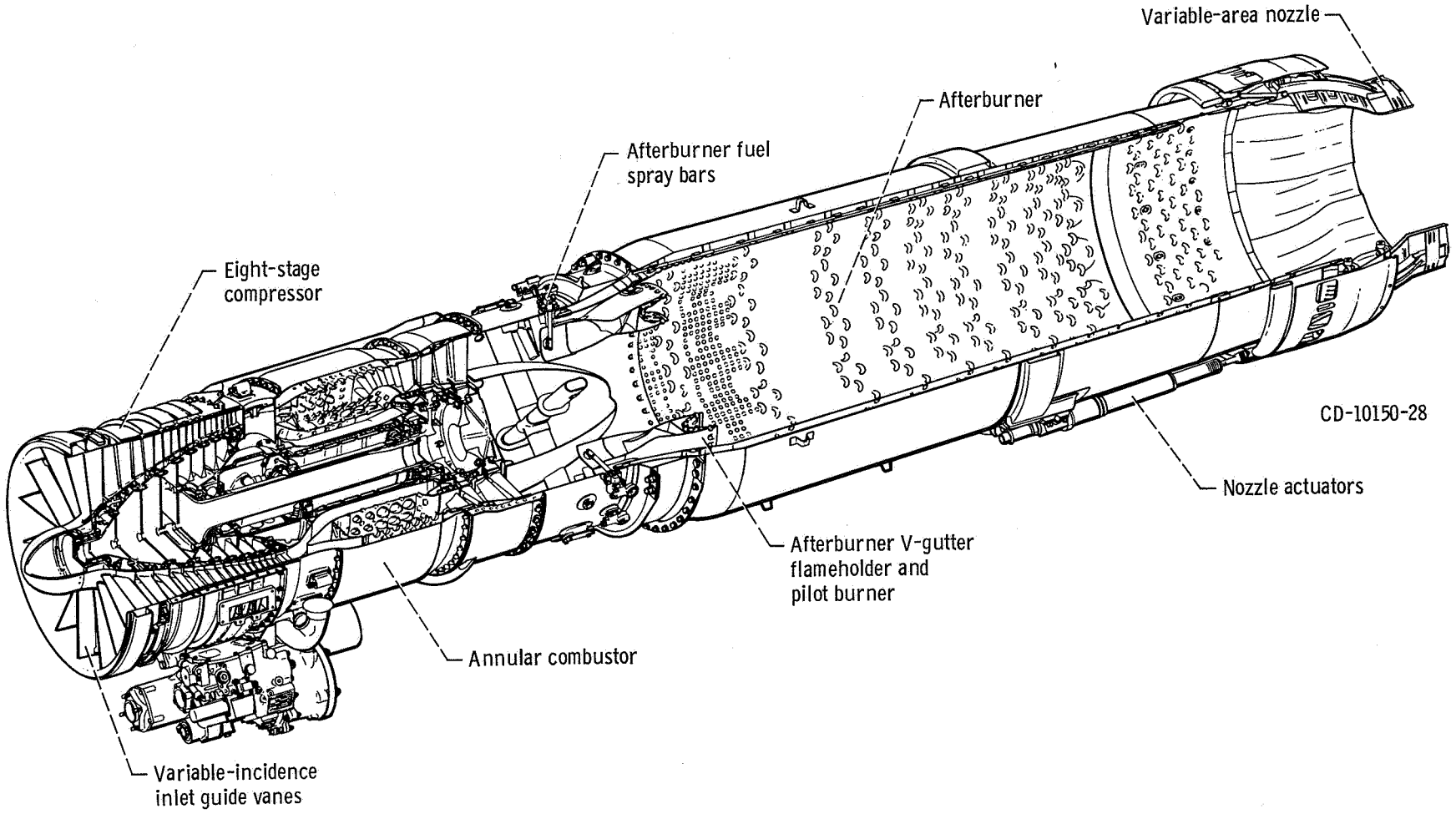

Figure 1. - Cutaway drawing of J85-GE-13 afterburning turbojet engine.

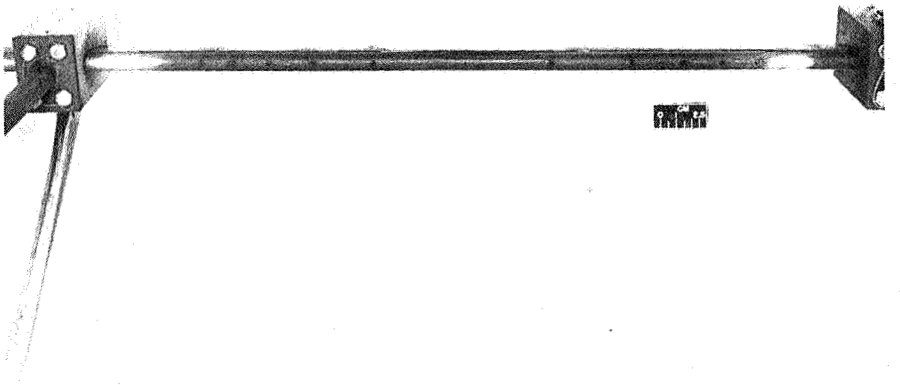

C-72-2338

Figure 2. - Water cooled gas sample rake sized to sample at maximum afterburning.

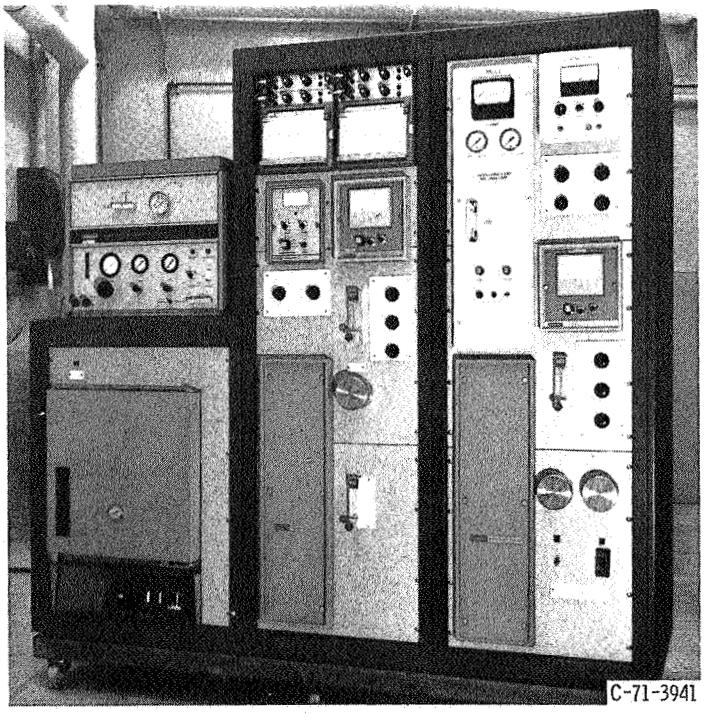

C-71-3941

Figure 3. - Exhaust gas analysis system instruments.

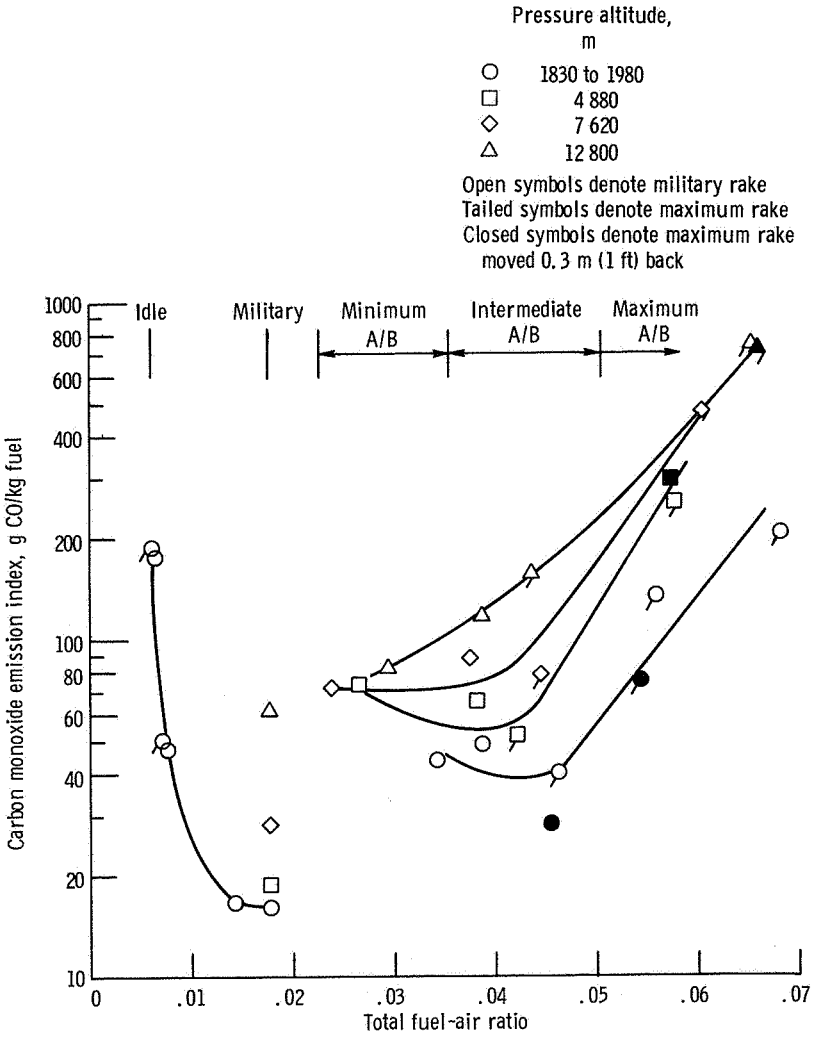

Figure 4. - Carbon monoxide emission index as a function of total fuel-air ratio at various pressure altitudes.

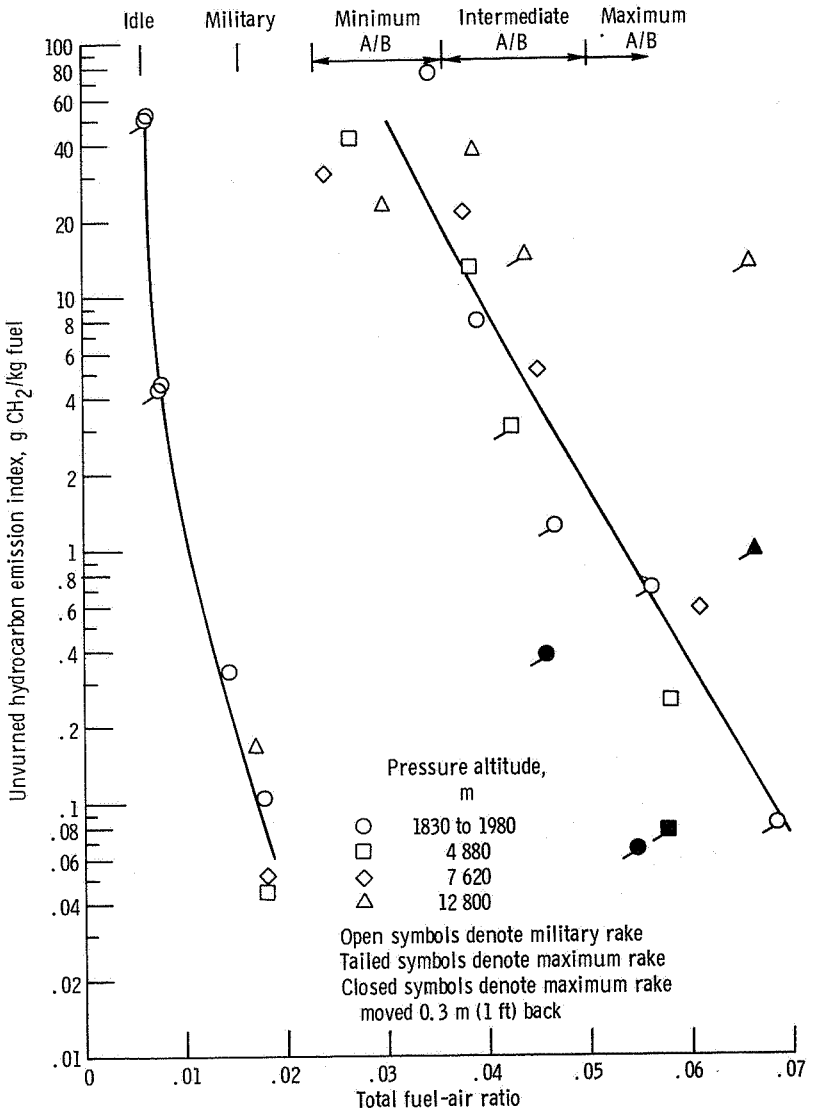

Figure 5. - Unburned hydrocarbon emission index as a function of total fuel-air ratio at various pressure altitudes.

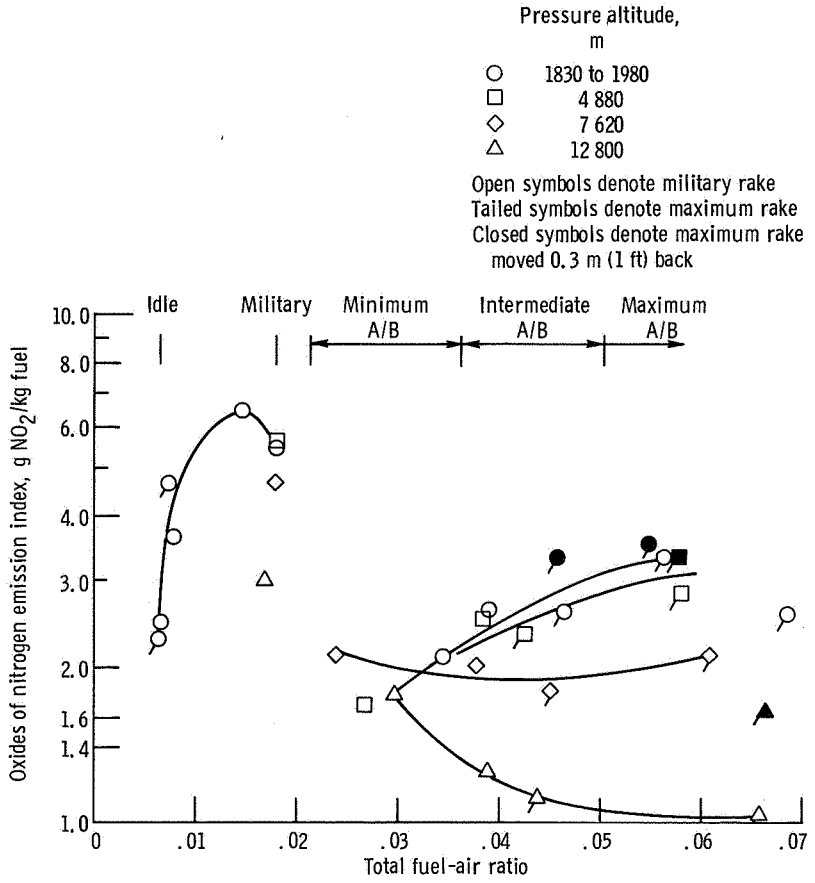

Figure 6. - Oxides of nitrogen emission index as a function of total fuel-air ratio at various pressure altitudes.

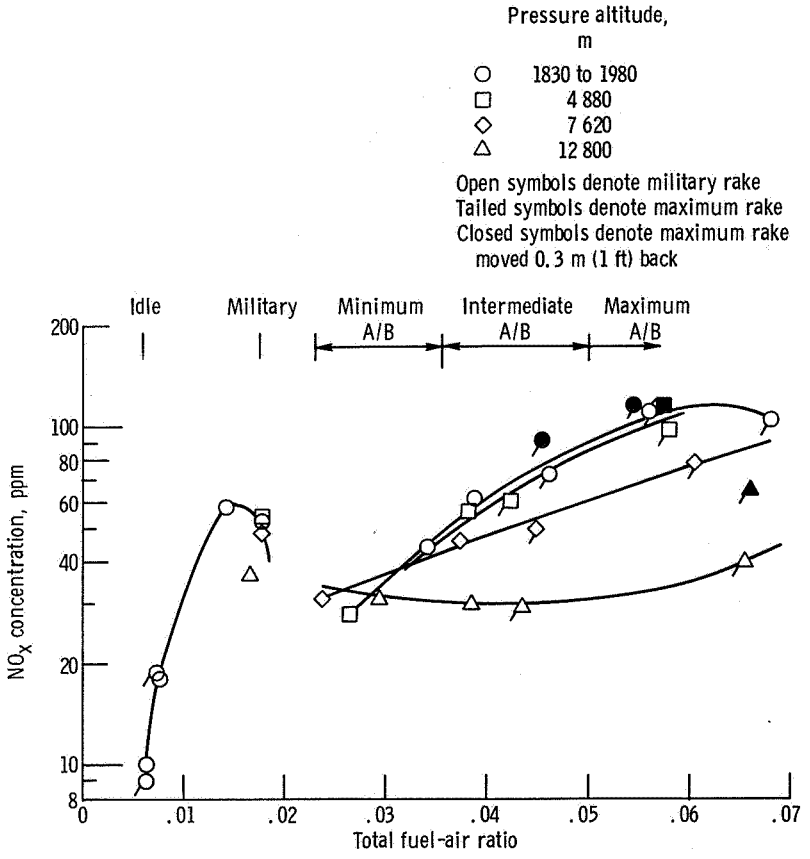

Figure 7. - Oxides of nitrogen concentration as a function of total fuel-air ratio at various pressure altitudes.

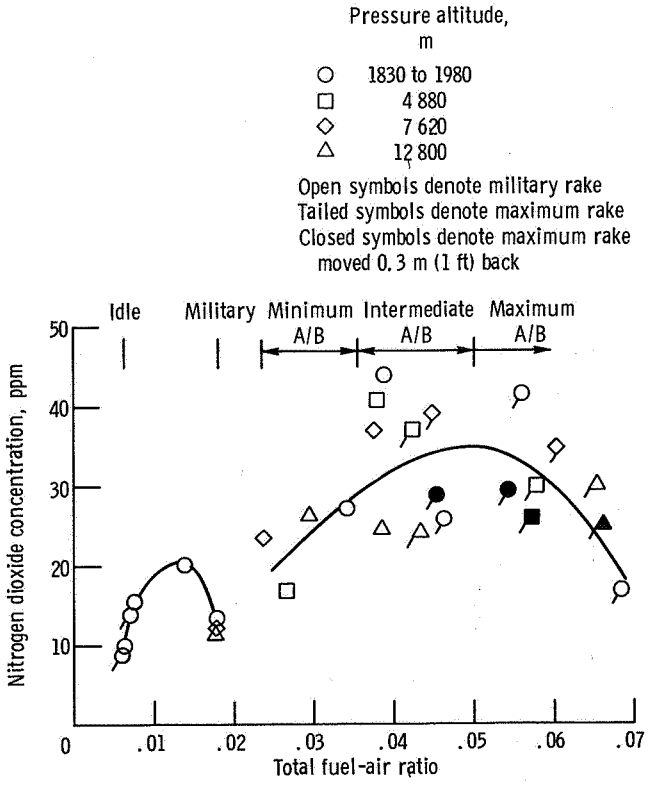

Figure 8. - Nitrogen dioxide concentration as a function of total fuel-air ratio at various pressure altitudes.

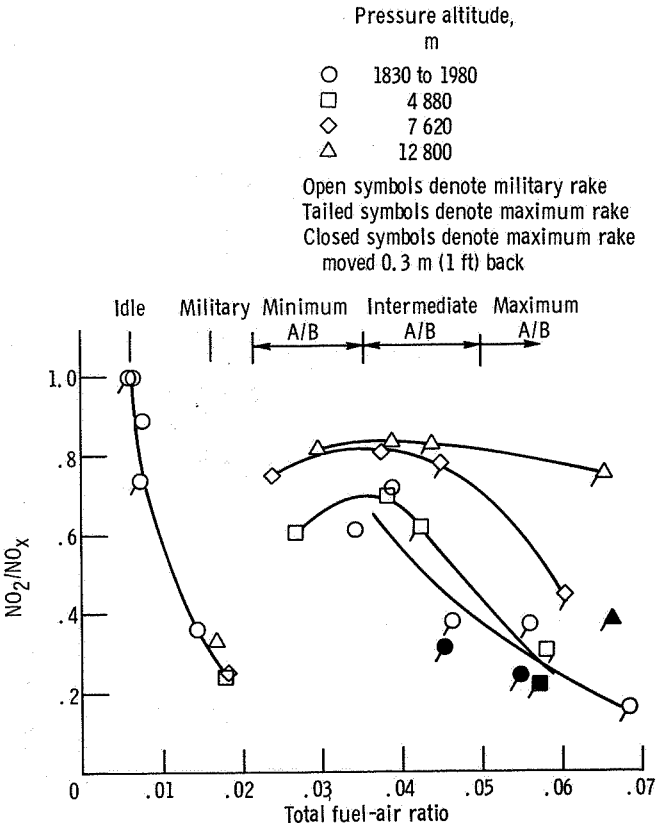

Figure 9. - Nitrogen dioxide fraction of total oxides of nitrogen as a function of total fuel-air ratio at various pressure altitudes.

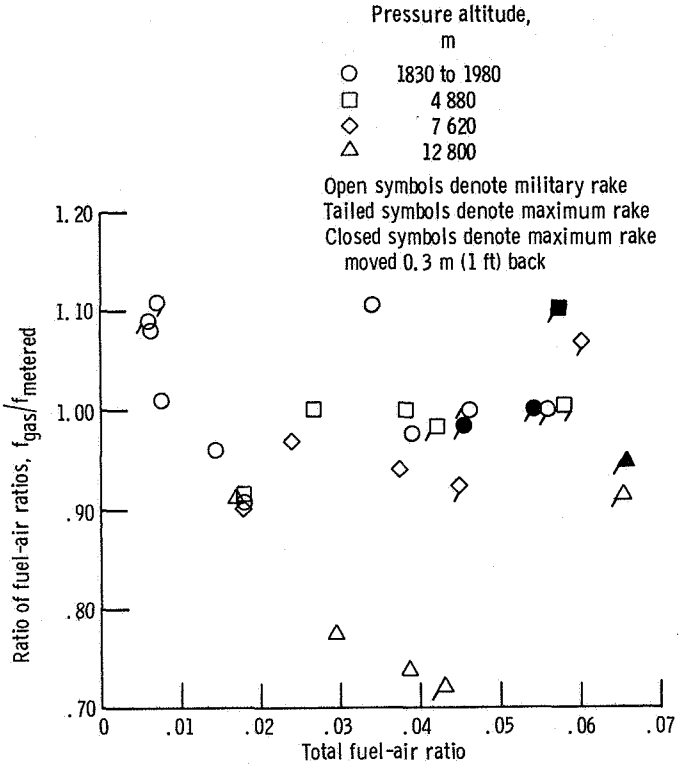

Figure 10. - Comparison of fuel-air ratios to check sample validity.

NASA-Langley, 1973 —— 33 E-7238